Interference, Fluctuation, and Alternation of Electron Tunneling in Protein Media. 1. Two Tunneling Routes in Photosynthetic Reaction Center Alternate Due to Thermal Fluctuation of Protein Conformation

Hirotaka Nishioka, Akihiro Kimura, and Takahisa Yamato

Department of Physics, Graduate School of Science, Nagoya University, Furo-cho, Chikusa-ku, Nagoya 464-8602, Japan

Tsutomu Kawatsu

Department of Chemistry, Duke University, Durham, North Carolina 27708-0349

Toshiaki Kakitani*

Department of General Education, Faculty of Science and Technology, Meijo University, Tenpaku-ku, Nagoya 468-8502, Japan

Received: August 18, 2004; In Final Form: November 5, 2004

Electron tunneling routes for the electron transfer from the bacteriopheophytin anion to the primary quinone in the bacterial photosynthetic reaction center of *Rhodobactor sphaeroides* are investigated by a combined method of molecular dynamics simulations for the protein conformation fluctuation and quantum chemical calculations for the electronic states of the donor, acceptor, and protein medium. The analysis of the tunneling route is made by mapping interatomic electron tunneling currents for each protein conformation. We found that there are two dominant routes mainly passing through Trp^{M252} (Trp route) or mainly passing through Met^{M218} (Met route). Actual electron tunneling pathways alternate between the two routes, depending on the protein conformation which varies with time. When either the Trp route or the Met route dominates, the electron tunneling matrix element $|T_{DA}|$ becomes large. When both the Trp route and the Met route dominate, $|T_{DA}|$ becomes very small due to the destructive interference of the electron tunneling currents between the two routes. We found that a linear relationship exists between the value of $|T_{DA}|$ and the inverse of the degree of destructive interference Q for a wide range of values (ca. $3-10^3$ for Q). A similar relationship was also found previously for electron transfer in ruthenium-modified azurins (Kawatsu, T.; Kakitani, T.; Yamato, T. *J. Phys. Chem. B* **2002**, *106*, 11356), suggesting that this relationship holds true in general. From these results, we are led to the conclusion that $|T_{DA}|$ cannot exceed a maximum value at $Q = 1$, even if much variation of $|T_{DA}|$ happens due to the fluctuation of protein conformation. We also conclude that the property of the electron transfer alternates between constructive and destructive interference, due to the fluctuation of protein conformation. It is impossible to keep a system in either constructive or destructive interference because thermal fluctuation of protein conformation takes place.

1. Introduction

Long-range electron transfers between protein cofactors play significant roles in biological functions such as photosynthesis and respiration.[1] The rate of the long-range electron transfer is usually written as follows[2]

$$k_{ET} = \frac{2\pi}{\hbar}|T_{DA}|^2(FC) \qquad (1)$$

where T_{DA} is the electron tunneling matrix element and (FC) is the thermally averaged Franck−Condon factor. In eq 1, Fermi's golden rule and the Condon approximation are used. Namely, T_{DA} is assumed to be independent of nuclear dynamics. The long-range electron transfer occurs via the superexchange mechanism where the electron tunnels use virtual states provided by protein environments.[3−5] Therefore, T_{DA} in the long-range electron transfer is controlled by the protein structure or protein conformation. Various methods for computation of T_{DA} by taking into account the protein structure have been presented.[6−13] The methods to determine the electron tunneling pathways such as the pathways model,[14−16] the tube model,[17−19] tunneling current analysis,[8,12,20−22] and the worm model[23] have given us significant insight into the quantum mechanical interference problem in long-range electron tunneling.

During these investigations, interest on the effect of thermal fluctuation of protein conformation on T_{DA} has grown.[24−28] This effect has often been investigated by the following computational approach. Molecular dynamics (MD) simulations are performed to reproduce the thermal fluctuation of protein conformation, and then T_{DA} is calculated by quantum chemistry for each snapshot of the MD simulations. These computational studies[24,25,28−32] have demonstrated that T_{DA} is strongly influenced by the thermal fluctuation of protein conformation. Daizadeh et al.[24] observed that the fluctuation of T_{DA} in

* Author to whom correspondence should be addressed. Phone: +81-52-838-2394. Fax: +81-52-832-1170. E-mail: kakitani@ccmfs.meijo-u.ac.jp.

10.1021/jp046282x CCC: $30.25
Published on Web 01/15/2005

ruthenium-modified azurin occurs on a short time scale (10−80 fs) and the sign of T_{DA} is also changed with thermal fluctuation, as discovered by a combined study of the MD simulations and quantum chemical calculations at an extended Hückel level. Wolfgang et al.[26] performed MD simulations to reproduce the thermal fluctuation of oligopeptides and then computed the matrix element of Green's function for oligopeptides using the CNDO/S level Hamiltonian for each configuration. They observed that the matrix element of Green's function changes in magnitude and sign with thermal fluctuation of protein conformation. Kawatsu et al.[30] demonstrated that the rapid fluctuation of T_{DA} is also seen in the six derivatives of ruthenium-modified azurins. Therefore, the rapid fluctuation of T_{DA} is a general property of electron tunneling in protein media. These results indicate that the Condon approximation is not valid for the long-range electron-transfer reaction in protein. It is expected that this kind of property of the nuclear dynamics will affect greatly the electron-transfer rate.

The effect of thermal fluctuation of protein conformation on T_{DA} is a problem relevant to the interference among the electron tunneling currents. Balabin and Onuchic[28] pointed out that T_{DA} is sensitive to nuclear dynamics when dominant tunneling tubes interfere destructively. They introduced a coherence parameter C, which is computed by a statistical average of T_{DA}. They proposed that C can be used as an indicator to judge whether the system is of constructive or destructive interference.[28]

In the present paper, we investigate the electronic tunneling matrix element T_{DA} for the electron transfer from the bacteriopheophytin (Bph) anion to the primary quinone (Q_A) in bacterial photosynthetic reaction center of *Rodobacter sphaeroides*. We performed a combined study of molecular dynamics simulations for the whole protein and quantum chemical calculations for the donor, acceptor, and protein media. We show how drastically the dominant electron tunneling routes are changed by the protein conformation change and how the destructive interference occurs. The present result is somewhat different from the result by Balabin and Onuchic.[28] We discuss a proper index for the interference problem in the electron tunneling through protein media.

2. Method

2.1. Molecular Dynamics Simulations and Electronic Structure Calculations. The molecular structure used in our molecular dynamics (MD) simulations consists of the whole protein of the reaction center of *Rodobacter sphaeroides* (PDB code 1AIJ).[33] The 262 water molecules incorporated in the structure 1AIJ are taken into account after optimization of their positions. Coulombic potentials over 12 Å are approximated by the PPPC method.[34] The MD program PRESTO[35] is used with the AMBER force field.[36] The harmonic restriction is imposed on the heavy atoms in the surface residues of the protein. The same restriction is imposed on oxygen atoms of water molecules. The system is kept at 300 K. The MD step size is 1 fs. After 160 ps of equilibration, we picked up a snapshot at every 50 fs for 15 ps. When we calculate T_{DA} for each protein conformation, we adopt the pruned protein, which consists of Bph, Q_A, and peptides that reside within 8 Å from the cofactors. We have confirmed that the residues other than the 60 amino acids have little influence on the value of T_{DA}.

The electronic states of the pruned protein are solved at the extended Hückel level. We refer to the FORTICON8 program for the extended Hückel calculations.[37] We use the ITPACK 2C[38] package for solving the secular equations. The electronic structures of the donor and the acceptor are calculated by the PM3 method.[39] We use the GAUSSIAN 98 package[40] for the PM3 program. Figure 1 shows truncated structures of Bph and Q_A molecules for the donor and acceptor, respectively. In the electron transfer from Bph^- to Q_A, the lowest unoccupied molecular orbital of the neutral Bph becomes the molecular orbital of the donor ϕ_D, and the lowest unoccupied molecular orbital of Q_A becomes the molecular of the acceptor ϕ_A. In such a treatment, ϕ_D and ϕ_A almost consist of π orbitals delocalized on the pheophytin and quinone ring, respectively. They are slightly extended to the σ orbitals of side chains. The residual parts of Bph and Q_A from the truncated structures are incorporated into the mediator. The value of T_{DA} is calculated by the pseudo-Greens' function technique[13,41,42] for each MD snapshot. The electron tunneling pathways are analyzed by drawing map of interatomic tunneling currents.[30]

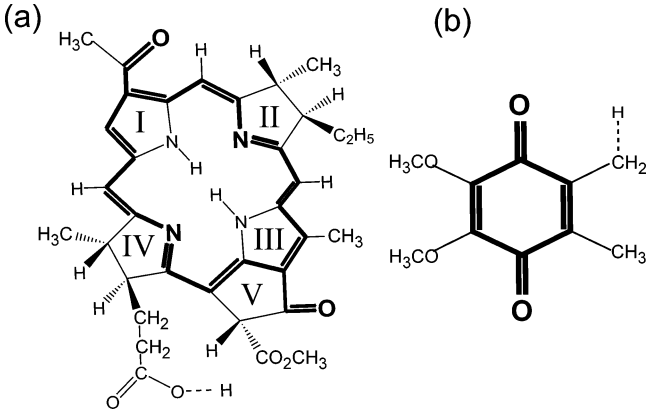

Figure 1. Chemical structures of (a) donor and (b) acceptor. The long hydrocarbon chains of the native bacteriopheophytin and the native ubiquinone are truncated down to a hydrogen atom. Bold lines represent the π-conjugated part.

2.2. Tunneling Matrix Elements and Interatomic Tunneling Currents. The theoretical derivation of the tunneling matrix element T_{DA} using the interatomic tunneling currents was given before.[8−13] The obtained formula is as follows

$$T_{DA} = \hbar \sum_{a \in \Omega_D^j, b \notin \Omega_D^j} J_{ab} \tag{2}$$

where J_{ab} is the interatomic tunneling current from atom a to atom b and Ω_D^j is a donor separated from the acceptor side by plane j. The interatomic tunneling current J_{ab} is expressed as follows

$$J_{ab} = \sum_{\mu \in a, \nu \in b} J_{\mu\nu} \tag{3}$$

$$J_{\mu\nu} = \frac{1}{\hbar}(C_\mu^i C_\nu^f - C_\mu^f C_\nu^i)(H_{\mu\nu} - ES_{\mu\nu}) \tag{4}$$

where C_μ^i and C_ν^i are the coefficients of atomic orbitals ϕ_μ and ϕ_ν in the molecular orbital Ψ_i of the initial state, respectively, C_μ^f and C_ν^f are the coefficients of atomic orbitals ϕ_μ and ϕ_ν in the molecular orbital Ψ_f of the final state, respectively, H is the one-electron Hamiltonian, S is the overlap integral, and E is the tunneling energy.

2.3. Coherence Parameter *C* and Degree of Destructive Interference *Q*. Balabin and Onuchic[28] have presented a coherence parameter C to represent the manner of destructive interference among the tunneling tubes in the system as follows

$$C = \frac{\langle T_{DA} \rangle^2}{\langle T^2_{DA} \rangle} \tag{5}$$

where $\langle\ \rangle$ represents the average over MD snapshots. They suggested that C is close to 1 when the destructive interference is rare, while it is close to 0 when the destructive interference is popular. It should be noticed that this parameter refers to the interference among different tunneling patterns corresponding to the different protein conformations. Therefore, it is assumed that the variety of T_{DA} is due to the different amounts of destructive interference among tunneling tubes.

On the other hand, Kawatsu et al.[30] proposed the other kind of parameter Q, called the degree of the destructive interference, as follows:

$$Q = \frac{1}{N}\sum_{j}^{N} Q_j \tag{6}$$

$$Q_j = \frac{\sum_{a\in\Omega_D^j} \sum_{b\notin\Omega_D^j} |J_{ab}|}{|\sum_{a\in\Omega_D^j} \sum_{b\notin\Omega_D^j} J_{ab}|} \equiv \frac{U_j}{|T_{DA}|} \tag{7}$$

where N is the total number of the sampling planes inserted between the donor and acceptor molecules. The degree of the destructive interference Q refers to the interference effect among interatomic tunneling currents on a map. The value of Q varies with the conformational change of protein. This Q value can be directly correlated with the T_{DA} value in each protein conformation.

2.4. Normalized Interatomic Tunneling Current. To map the interatomic tunneling currents for convenience of comparison of the maps with different values of Q, we define a normalized interatomic tunneling current $\bar{K}_{ab}$ as follows[30]

$$\bar{K}_{ab} = \frac{1}{Q}\frac{\hbar J_{ab}}{|T_{DA}|} \tag{8}$$

The map represented by the use of $\bar{K}_{ab}$ evidently shows how the tunneling currents are flowing, gathering, dispersing, and circulating for each value of Q.

3. Results

3.1. Rapid and Large Fluctuation of T_{DA}. Figure 2 shows an example of the time dependence of the calculated value of T_{DA} at every 50 fs for the electron tunneling from Bph^- to Q_A, for three kinds of tunneling energies −9.0, −9.5, and −10.0 eV, which are the candidate values in this system.[28] The sign of T_{DA} changes rapidly. Since the donor−acceptor location does not change significantly within such a short time, this rapid change of T_{DA} is caused by delicate conformation changes of the protein. We see that T_{DA} values calculated for the three tunneling energies fit each other very well at almost all of the times. We use −9.5 eV tunneling energy hereafter.

3.2. Two Main Tunneling Routes. In previous works, Kawatsu et al. developed a novel method to analyze the electron tunneling route by mapping interatomic tunneling currents.[23,43] Here, we used the name "route" because we found that a group of tunneling currents is properly expressed by connection of some blocks of a considerable number of heavy atoms. Therefore, the concept of the route is more bulky than the concept of the pathways[14,15] or the tubes.[17−19] In the present

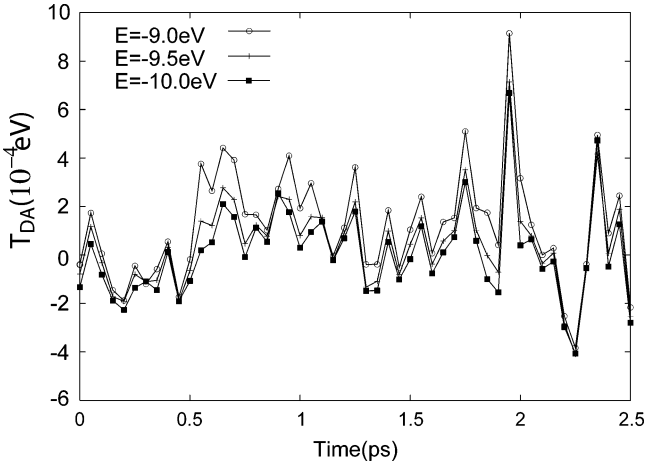

Figure 2. Time dependence of T_{DA} for three different tunneling energies (E = −9.0, −9.5, and −10.0 eV). The value of T_{DA} is computed using the protein conformation at every 50 fs for 2.5 ps.

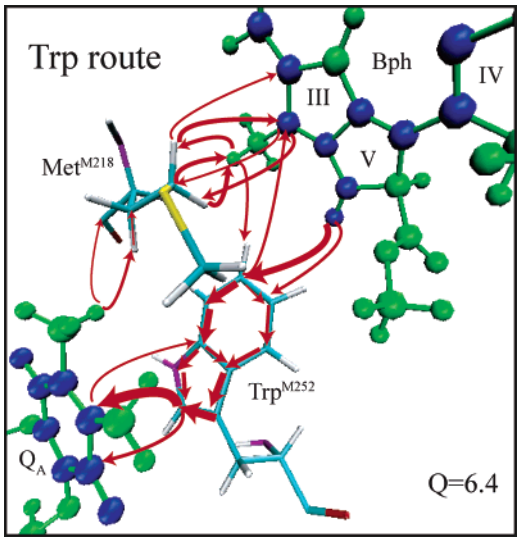

Figure 3. Map of the normalized interatomic tunneling current $\bar{K}_{ab}$ in the case of $Q = 6.4$. Only interatomic tunneling currents for $\bar{K}_{ab} > 0.4$ are shown by red arrows whose widths are roughly proportional to the value of $\bar{K}_{ab}$. The blue and green balls indicate the atoms constituting the donor and the acceptor. The blue ball indicates the atoms constituting the π-conjugated part in the donor or the acceptor molecule. The atomic view is produced with use of VMD.[44]

analysis, we drew various $\bar{K}_{ab}$ maps for different protein conformations. After drawing the maps, we found that the large interatomic tunneling currents dominantly flow through the two amino acids Trp^{M252} and Met^{M218}. Maps of three typical cases are shown in Figures 3, 4, and 5. Figure 3 is the case where the tunneling currents flow mostly through Trp^{M252} almost from donor to acceptor. We call this group of tunneling currents the "Trp route". In this case, T_{DA} is positively large and Q is small. Figure 4 is the case where the tunneling currents flow mostly through Met^{M218} almost from acceptor to donor. We call this group of tunneling currents the "Met route". In this case, T_{DA} is negatively large and Q is small. Figure 5 is the case where the tunneling currents flow through Trp^{M252} and Met^{M218} almost in a circular way between donor and acceptor. In this case, $|T_{DA}|$ is small and Q is large. This last one is a typical case where the destructive interference occurs between the Trp route and the Met route. As a result, we found that the two main routes (Trp route and Met route) work independently or work in a manner of destructive interference for the electron tunneling. Here, it should be pointed out that His^{M219}, which is the next amino

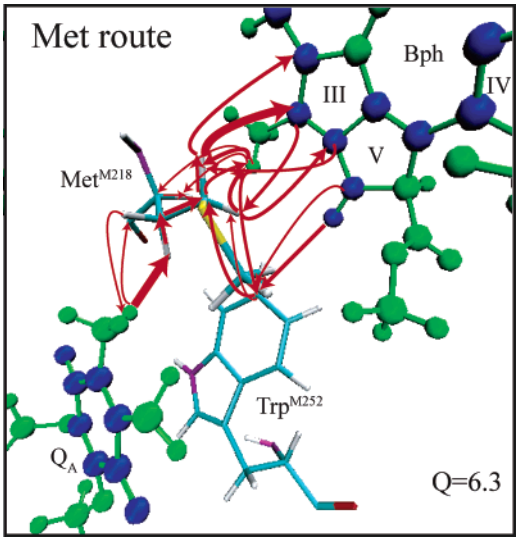

Figure 4. Map of the normalized interatomic tunneling currents in the case of $Q = 6.3$. Only the interatomic tunneling currents for $\bar{K}_{ab} > 0.4$ are shown. Notation is the same as in Figure 3.

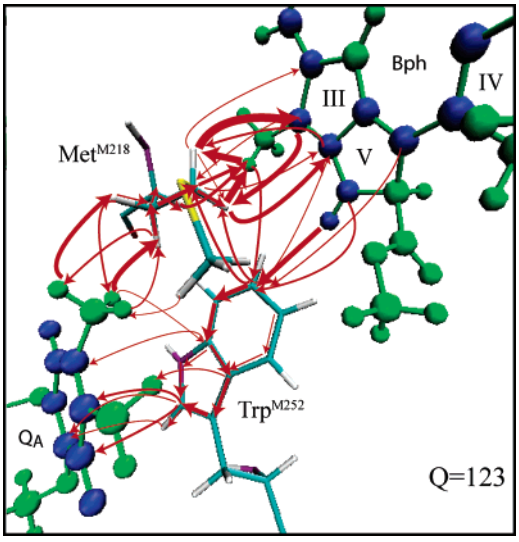

Figure 5. Map of the normalized interatomic tunneling currents in the case of $Q = 123$. Only the interatomic tunneling currents for $\bar{K}_{ab} > 0.2$ are shown. Notation is the same as in Figure 3.

acid to Met^{M218}, affects considerably the interatomic tunneling currents through Met^{M218} even though the interatomic tunneling currents through His^{M219} are very small. Namely, His^{M219} works indirectly in the electron tunneling current through the Met route. Therefore, the three amino acids Trp^{M252}, Met^{M218}, and His^{M219} play a significant role in the electron transfer from Bph$^-$ to Q_A. These three amino acids were adequately chosen in the previous work.[28]

3.3. $|T_{DA}|$ is Proportional to Q^{-1}. In Figure 6A, we plotted the logarithm of $|T_{DA}|$ as a function of the logarithm of Q for 301 protein configurations at every 50 fs. We see that the value of Q widely distributes between 3 and 1000. The densely distributed region of Q is 5−50. The value of $|T_{DA}|$ is also widely distributed from about 8×10^{-4} to 10^{-6} eV. We also see that a good linear relation holds between log $|T_{DA}|$ and log Q with a slope of approximately −1. We find that the correlation coefficient η is −0.956. It should be noticed that η is −1.00 when all of the points are on the line log $|T_{DA}|$ = const − log Q. Therefore, we can say that the correlation of $|T_{DA}|$ proportional to Q^{-1} is very good. This kind of relationship was also observed in the six derivatives of ruthenium-modified azurin systems before.[30] Because the protein environment of the reaction center is quite different from that of azurin, we may conclude that the linear relationship ($|T_{DA}| \propto Q^{-1}$) holds true for general electron transfer in protein environments.

We investigate the reason such a simple, linear relationship is obtained. For this purpose, we make a stronger pruning of the protein. We consider three other kinds of pruned proteins: (1) three amino acids Trp^{M252}, Met^{M218}, and His^{M219} (Trp^{M252} + Met^{M218} + His^{M219} system), (2) one amino acid Trp^{M252} (Trp^{M252} system), and (3) two amino acids Met^{M218} and His^{M219} (Met^{M218} + His^{M219} system). The coordinates of these amino acids are taken from the MD simulation data, which were obtained by considering all of the amino acids in the reaction center. Bph$^-$ and Q_A are considered in the same positions as the case for the 60 amino acids. The calculated results of $|T_{DA}|$ and Q for these three systems are shown in Figure 6, parts B, C, and D. The graph of the Trp^{M252} + Met^{M218} + His^{M219} system in Figure 6B shows that a clear relationship between log $|T_{DA}|$ and log Q holds true with a slope of approximately −1 (correlation coefficient η is −0.935). Namely, a good linear relationship between $|T_{DA}|$ and Q^{-1} holds true, and it is quite similar to that of Figure 6A, which was obtained by considering 60 amino acids. The graph of the Trp^{M252} system in Figure 6C shows that most of the points are in the narrow range of Q_A and $|T_{DA}|$, and no correlation is obtained between $|T_{DA}|$ and Q (the correlation coefficient η is as low as −0.679). The graph of the Met^{M218} + His^{M219} system in Figure 6D shows an intermediate property between Figures 6B and 6C. Considerable numbers of points are in the narrow range of Q and $|T_{DA}|$. However, some points are distributed over the large values of Q and small values of $|T_{DA}|$ (the correlation coefficient η is −0.924). From these results, we conclude that pruning the protein to one amino acid or one route for the tunneling pathway is not appropriate in this system. On the other hand, so far as the linear relationship between $|T_{DA}|$ and Q^{-1} is concerned, the pruned protein consisting of the three amino acids (Trp^{M252}, Met^{M218}, and His^{M219}) can play a sufficient role as a tunneling mediator, comparable to the native protein.

In Table 1, we list the calculated values of $\langle T_{DA}^2 \rangle$, C, $\langle Q \rangle$, and η for the different pruned proteins. Especially, we added the data for a system of 13 amino acids, which neatly surrounds donor and acceptor molecules. Here, we must mention the following. In the 60 amino acid system, the phytyl group of Bph and the phytol group of ubiquinone are involved in the mediator. In the 13 amino acid system, the phytol group of ubiquinone is involved in the mediator. From Table 1, we find that the coherence parameter C is large for the one amino acid systems Trp^{M252} and Met^{M218}, respectively, but that it is very small for the systems of more than three amino acids. On the other hand, the value of $\langle Q \rangle$ is small for the Trp^{M252} system, rather large for the Met^{M218} system, and large for the systems of more than two amino acids. Therefore, there is roughly a qualitative tendency for C to be large when $\langle Q \rangle$ is large. The value of $\langle T_{DA}^2 \rangle$ is the largest for the Met^{M218} system and smallest for 60 amino acid system. We notice that values of C and $|T_{DA}|^2$ for the 13 amino acid system are very close to those for the 60 amino acid system and are a little smaller than those for the Trp^{M252} + Met^{M218} + His^{M219} system. The correlation coefficient η is close to −1 for the systems of 60 amino acids, 13 amino acids, and Trp^{M252} + Met^{M218} + His^{M219}. The value of η becomes small as the number of the amino acids becomes small. Among them, the value of η for the Trp^{M252} system is the smallest. The reason that the value of η of the Trp^{M252} system is so small will be due to a rigid conformation of the Trp residue.

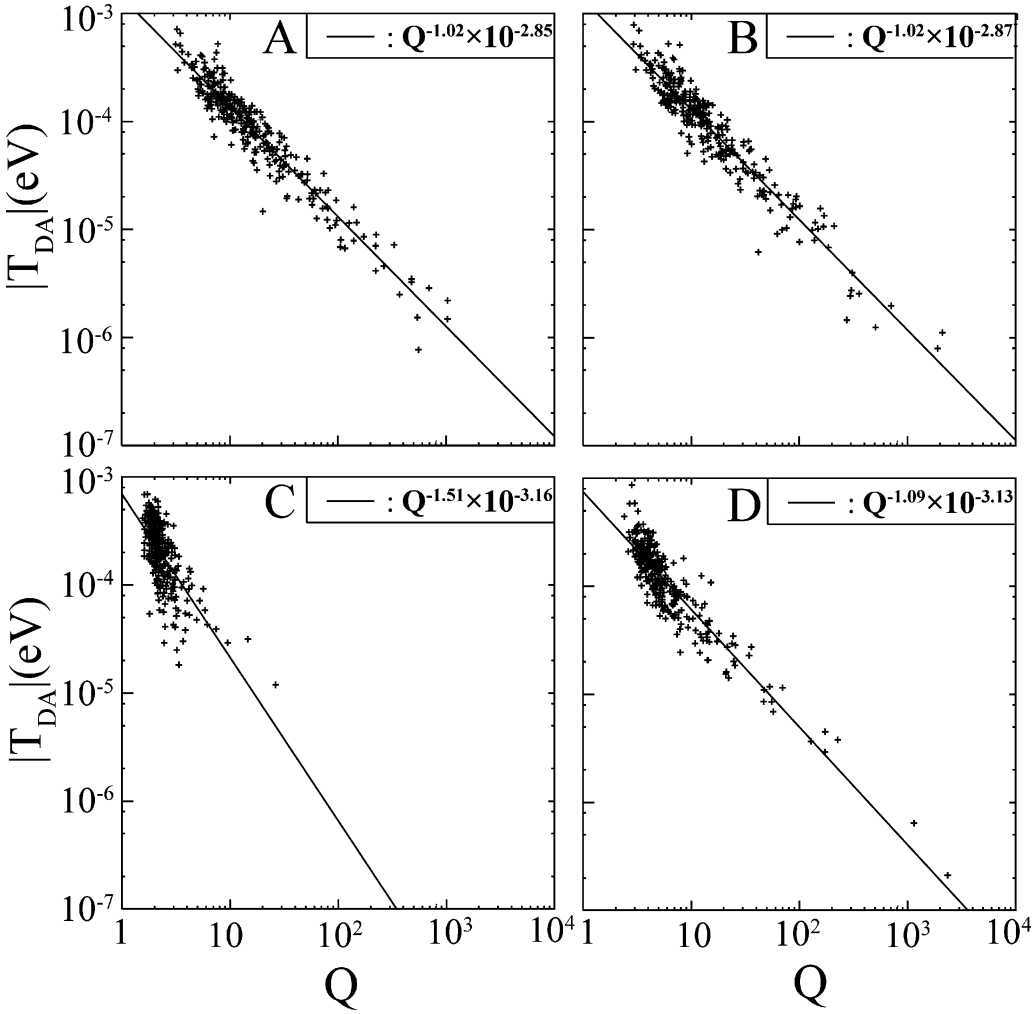

Figure 6. Correlation between the absolute value of the electron tunneling matrix element $|T_{DA}|$ and the degree of destructive interference Q. The following four kinds of pruned proteins are considered: (A) 60 amino acids, (B) $Trp^{M252} + Met^{M218} + His^{M219}$, (C) Trp^{M252}, and (D) $Met^{M218} + His^{M219}$. The straight line represents the least-squares fitting line for the relation between log $|T_{DA}|$ and log Q.

TABLE 1: Calculated Values of $\langle T_{DA}^2 \rangle$, C, $\langle Q \rangle$, and η for the Six Kinds of Systems: 60 Amino Acid, 13 Amino Acid, $Trp^{M252} + Met^{M218} + His^{M219}$, $Met^{M218} + His^{M219}$, Met^{M218}, and Trp^{M252}

system	$\langle T_{DA}^2 \rangle$ (10^{-7} eV^2)	C	$\langle Q \rangle$	η
60 amino acids	0.282	0.0479	42.1	−0.956
13 amino acids	0.285	0.0463	41.0	−0.955
$Trp^{M252} + Met^{M218} + His^{M219}$	0.317	0.0665	44.0	−0.953
$Met^{M218} + His^{M219}$	0.323	0.618	21.1	−0.924
Met^{M218}	0.905	0.524	11.2	−0.874
Trp^{M252}	0.749	0.752	2.49	−0.679

It appears that a high correlation coefficient is obtained when the conformation of the protein is flexible.

3.4. Fluctuation of Sign and Amplitude of T_{DA}. Next, we investigate how the sign and the amplitude of T_{DA} is changed with time. In Figure 7A, we plot T_{DA} calculated by using the Trp^{M252} system (red line) by using the $Met^{M218} + His^{M219}$ system (green line) as a function of time. We see that both the red lines and the green lines fluctuate very quickly. Almost all of the points of the red line reside in the positive region of T_{DA}, while almost all of the points of the green line reside in the negative region of T_{DA}. Therefore, the direction of the total tunneling current is opposite between the Trp^{M252} system and the $Met^{M218} + His^{M219}$ system. This property must be the origin of the destructive interference in the whole protein system. In the following, we confirm it.

In Figure 8, we plotted a correlation diagram of log $|T_{DA}^{Trp+Met+His}|$ vs log $|T_{DA}^{Trp} + T_{DA}^{Met+His}|$ with the + symbol. Here, $T_{DA}^{Trp+Met+His}$, T_{DA}^{Trp}, and $T_{DA}^{Met+His}$ are the tunneling matrix elements calculated using the $Trp^{M252} + Met^{M218} + His^{M219}$ system, Trp^{M252} system, and $Met^{M218} + His^{M219}$ system, respectively. Now, we define a parameter A as follows

$$A \equiv \left| \frac{T_{DA}^{Trp+Met+His}}{T_{DA}^{Trp} + T_{DA}^{Met+His}} \right| \tag{9}$$

When $A = 1$ holds, a simple additivity rule that $T_{DA}^{Trp} + T_{DA}^{Met+His} = T_{DA}^{Trp+Met+His}$ holds true. When A deviates from 1, such a simple additivity rule does not hold. In Figure 8, the bold line represents the case of $A = 1$. The two broken lines represent the cases for $A = 3$ and $1/3$, respectively. We find that 78.4% of the calculated points reside in the region between the two broken lines of $A = 3$ and $1/3$. (We also find that 63.1% of the calculated points reside in the region of A between 2 and $1/2$). There is a clear tendency that the points with the largest values of $T_{DA}^{Trp} + T_{DA}^{Met+His}$ are almost on the line $A = 1$. As the values of $T_{DA}^{Trp+Met+His}$ become small, the number of points that deviate largely from the line $A = 1$ increases.

Physical meaning of the above additivity rule that holds true for $A = 1$ is as follows. The electron tunneling currents through the Trp route, which is produced when only Trp^{M252} is

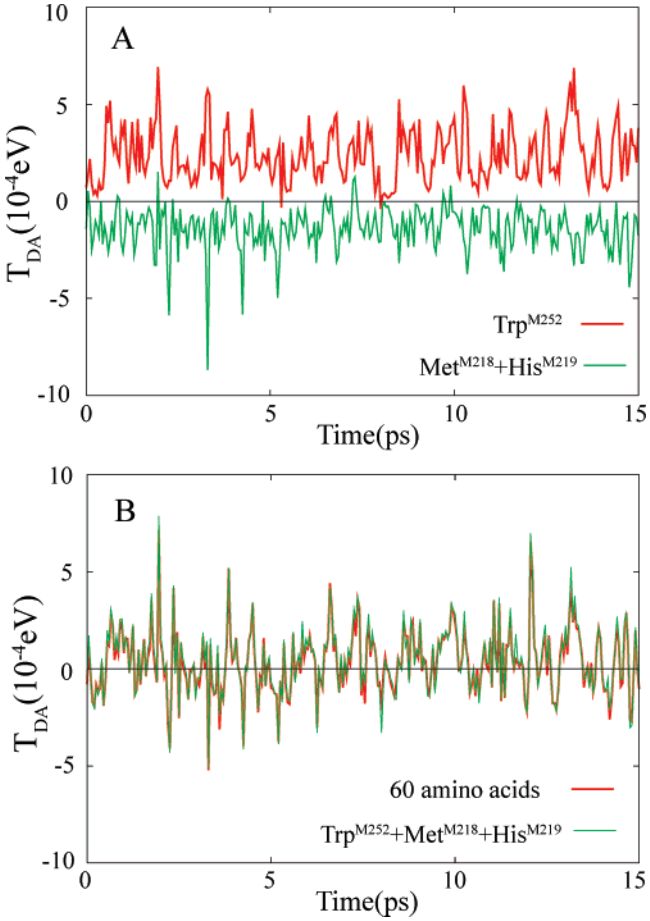

Figure 7. (A) Time dependence of the tunneling matrix element T_{DA} calculated for Trp^{M252} (red) and Met^{M218} + His^{M219} (green) systems. (B) Time dependence of T_{DA} calculated for 60 amino acid (red) and Trp^{M252} + Met^{M218} + His^{M219} (green) systems.

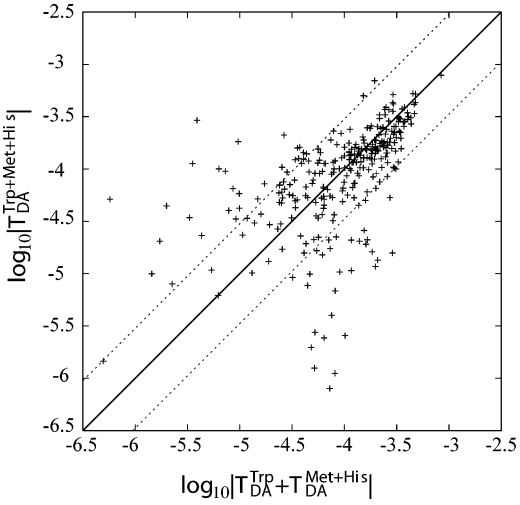

Figure 8. Plot of log $|T_{DA}^{Trp+Met+His}|$ vs log $|T_{DA}^{Trp} + T_{DA}^{Met+His}|$ for the 301 points of protein conformations. The bold line represents the case where $A \equiv |T_{DA}^{Trp+Met+His}|/|T_{DA}^{Trp} + T_{DA}^{Met+His}| = 1$ holds. The broken lines represent the cases where $A \equiv 3$ and $^1/_3$.

considered, are not affected by the amino acids in the Met route (Met^{M218} and His^{M219}). The electron tunneling currents through the Met route, which is produced when only Met^{M218} and His^{M219} are considered, are not affected by the amino acid in the Trp route (Trp^{M252}). Therefore, it happens that the T_{DA} of the Trp route cancels out the T_{DA} of the Met route when both routes are used simultaneously. The closer the point to the line of $A = 1$, the more completely the cancellation happens. Those points that greatly deviate from the additivity rule indicate that the electron tunneling currents through the Trp route are considerably affected by the amino acids in the Met route and vice versa. Figure 8 indicates that the additivity rule roughly holds when $|T_{DA}^{Trp} + T_{DA}^{Met+His}|$ is large, while the additivity rule is broken when $|T_{DA}^{Trp} + T_{DA}^{Met+His}|$ is small.

Next, we investigate how much the Trp^{M252} + Met^{M218} + His^{M219} system can substitute for the 60 amino acid system in the electron tunneling. In Figure 7B, we plotted T_{DA} as a function of time for the 60 amino acid system (red line) and the Trp^{M252} + Met^{M218} + His^{M219} system (green line). Since this plot is a linear scale for the amplitude of T_{DA}, the point of large value is more evident. The green curve in Figure 7B is almost the sum of the red curve and the green curve in Figure 7A, suggesting that a simple additivity rule approximately holds true for the larger values of T_{DA} in this three amino acid system. In Figure 7B, we find that the red curve fits the green curve very well in both the positive and negative regions of T_{DA}. This fact indicates that the Trp route of the three amino acid system remains almost the same as that of the 60 amino acid system when the Trp route is dominantly used. Similarly, the Met route of the three amino acid system remains almost the same as that of 60 amino acid system when the Met route is dominantly used.

4. Discussion

4.1. Reasoning of Discussing the Rapid Time Course of T_{DA}. In the present paper, we investigated the mechanism of rapid fluctuation of the electron tunneling matrix element T_{DA}. Typically, T_{DA} fluctuates in less than 50 fs with an amplitude on the order of 0.1 meV. According to the uncertainty principle of quantum mechanics between time and energy, an inequality $\Delta t \Delta E \geq \hbar$ should be satisfied, where $\hbar$ is Planck's constant divided by 2π. If one sets $\Delta t = 50$ fs and $\Delta E = 0.1$ meV, one obtains $\Delta t \Delta E = 8 \times 10^{-3}\ \hbar$. In such a case, apparently the inequality of the uncertainty principle is not satisfied in our system, and the discussion of the time course of T_{DA} is meaningless. However, it should be pointed out that T_{DA} is not an observable quantity, since it is a nondiagonal term of the Hamiltonian. It can even be a complex number in a certain representation of the electronic wave function. Therefore, substitution of T_{DA} into ΔE in the uncertainty principle is not allowed. In the second paper in this series of study, $T_{DA}(t)$ will be used in a form of the time correlation function $\langle T_{DA}(t) T_{AD}(0) \rangle$ to calculate the electron-transfer rate within the framework of the Fermi's golden rule, in a similar method to Rossky et al.[45,46] So far as we discuss the effect of the fluctuation of $T_{DA}(t)$ within the framework of Fermi's golden rule, the restriction by the uncertainty principle does not matter. Under such a situation, we should mention the reason that we plotted $|T_{DA}|$ as a function of Q and why we drew the map of the interatomic tunneling current J_{ab} in this paper even though $|T_{DA}|$, Q, and J_{ab} are not observable. These parameters are used so that the tunneling pathways can be visualized clearly and we can uncover the specific mechanism of the electron tunneling through protein media. Let us remember the fact that the spatial representation of the electronic wave function, which is not observable, is quite useful for discussion of the chemical bond.

4.2. Physical Meaning of the Linear Relationship between $|T_{DA}|$ and Q^{-1}. We have shown that a linear relationship approximately holds true between $|T_{DA}|$ and Q^{-1} over a large range of Q values for the electron transfer from Bph^- to Q_A in the photosynthetic reaction center. We already showed that the similar relationship also holds true for the electron transfer from

Cu^+ to Ru^{3+} in the six derivatives of ruthenium-modified azurin.[30] The above relationship may be common in the electron transfer through protein media.

With the same notations as the previous paper,[30] $|T_{DA}|$ is written as

$$|T_{DA}| = \frac{U}{Q} \tag{10}$$

where

$$U = \frac{1}{N}\sum_j U_j \tag{11}$$

and U_j is defined in eq 7. U_j represents the sum of absolute values of interatomic currents passing through the plane j. The parameter U is an average of U_j over the N planes. The linear relationship between $|T_{DA}|$ and Q^{-1} indicates that U is a constant value independent of the conformational fluctuation of proteins. The value of U is dominantly determined by the distance R_{DA} between the donor and acceptor[30,47,48] and partly determined by the secondary structures and their arrangement in the protein.[49] Some evidence for these concepts was provided in Figure 1 of ref 30, where correlation diagrams between log $|T_{DA}|$ and R_{DA} were shown in the course of fluctuation of protein conformation for the six derivatives of ruthenium-modified azurin. In the actual calculation using eq 11, U changes a little from map to map. Therefore, the coefficient U in the discussion of the linear relationship between $|T_{DA}|$ and Q^{-1} is an average of U over the various maps.

To understand the physical meaning of the linear relationship in more detail, we adopt a model that the system is composed of some routes and that each route is composed of many channels. The amplitude and direction of the tunneling current through each channel can vary with the conformational fluctuation of the protein. In the following discussion, however, we adopt only two routes and each route is composed of two channels, for simplicity. In Figure 9, we draw some cases of the tunneling currents for each route that would be important in our system. In case a, both of the two tunneling currents J_1 and J_2 flow constructively from donor (D) to acceptor (A) through route I. In case b, one tunneling current J_3 flows from D to A through route I, while the other tunneling current J_4 flows from A to D. In case c, both of the two tunneling currents J_5 and J_6 flow constructively from A to D through route II. In case d, one tunneling current J_7 flows from D to A through route II, while the other tunneling current J_8 flows from A to D. The contributions to T_{DA} and U from the route I are represented as T_{DA}^{I} and U^{I}, respectively, and are written in the figure. Contribution from route II is also written.

The route I is always open unless both J_1 and J_2 are small in case a. Route I is closed when $J_3 = J_4$ holds in case b. Route I is also closed when J_3 and J_4 are small. Similarly, route II is always open in case c. Route II is closed when $J_7 = J_8$ holds in case d. Route II is also closed when J_7 and J_8 are small. Since U is constant, we obtain

$$U/\hbar \equiv J_1 + J_2 + J_5 + J_6 = J_1 + J_2 + J_7 + J_8 = J_3 + J_4 + J_5 + J_6 = J_3 + J_4 + J_7 + J_8 \tag{12}$$

Using these relations, we obtain roughly the following relationships

$$U \equiv |T_{DA}(a)| \quad \text{or} \quad |T_{DA}(c)| > |T_{DA}(a+d)| \quad \text{or} \quad |T_{DA}(b+c)| > |T_{DA}(b+d)| \quad \text{or} \quad |T_{DA}(a+c)| \tag{13}$$

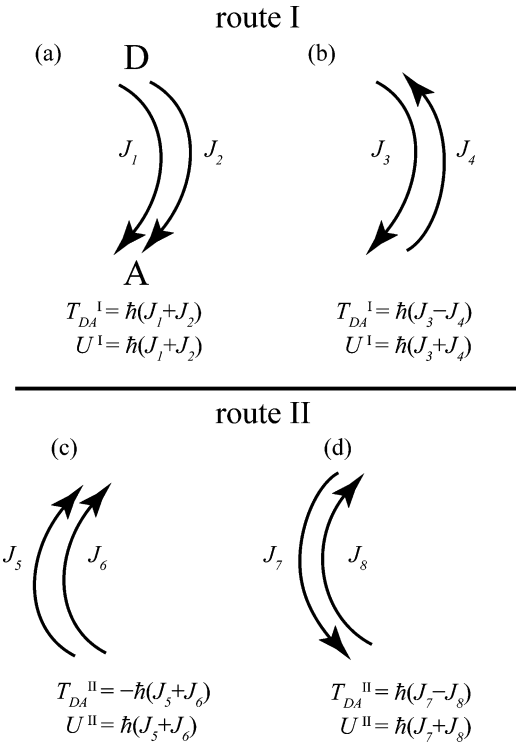

Figure 9. Schematic representation of the maps of tunneling currents through two routes each of which is composed of two channels. The arrow indicates the direction of the tunneling current. The value of J_i represents the amplitude of the tunneling current. Contribution to T_{DA} and U from the route I is represented as T_{DA}^{I} and U^{I}, respectively, and vice versa.

where $T_{DA}(a)$ indicates $T_{DA}^{I}(a) + T_{DA}^{II}(d)$ with $J_7 = J_8 = 0$, $T_{DA}(c)$ indicates $T_{DA}^{II}(c) + T_{DA}^{I}(b)$ with $J_3 = J_4 = 0$, $T_{DA}(a+c)$ indicates $T_{DA}^{I}(a) + T_{DA}^{II}(c)$, and so on. The above equation has a significant physical meaning. When multiple channels exist, the value of T_{DA} approaches the maximum value only when the directions of tunneling currents are the same. From the value of Q, we can estimate how much the direction of the tunneling currents are same. When the value of Q is close to 1, almost all of the tunneling currents have the same direction (constructive interference). When the value of Q is much larger than 1, the sum of the tunneling currents in the forward direction is nearly same as the sum of the tunneling currents in the backward direction (destructive interference). If we look at Figure 6, then the distribution of the value of Q is wide when a considerable number of amino acids are used as a mediator (60 amino acid system and $Trp^{M252} + Met^{M218} + His^{M219}$ system). When one or two amino acids are used as a mediator (Figure 6, parts C and D), the distribution of the value of Q is rather narrow and mostly in the range 2−5 (Trp^{M252} system) or 3−8 ($Met^{M218} + His^{M219}$ system). In the actual situation of a protein, it will be almost impossible to confine the mediator to one amino acid since the molecular size of donor and acceptor is large. In general, the value of Q distributes widely as shown in Figure 6, parts A or B. This fact indicates that the property of electron transfer alternates between constructive interference (small Q) and destructive interference (large Q), depending on the fluctuation of protein conformation. In other words, it is impossible to keep a system in either constructive or destructive interference, so far as the thermal fluctuation of protein conformation takes place.

Using Figure 9, we reinterpret Figures 3−5. In Figure 3, large tunneling currents flow from D to A through the Trp route, while only small tunneling currents flow from A to D through the

Met route. Therefore, the Trp route is open and corresponds to the case a with large values of J_1 and J_2. The Met route is almost closed and corresponds to the case c with small values of J_5 and J_6 or the case d with small values of J_7 and J_8. It is not the case for destructive interference that J_7 and J_8 are large with almost the same values in case d. In Figure 4, large tunneling currents flow from A to D through the Met route, while almost no tunneling current flows from D to A through the Trp route. Therefore, the Met route is open and corresponds to the case c with large values of J_5 and J_6. The Trp route is almost closed and corresponds to the case a with small values of J_1 and J_2 or the case b with small values of J_3 and J_4. It is not the case for destructive interference that J_3 and J_4 are large with almost the same values in case b. In Figure 5, large tunneling currents flow from D to A through the Trp route, and large tunneling currents flow from A to D through the Met route. Therefore, both the Trp route and the Met route are open with large values of J_1 and J_2 in case a and large values of J_5 and J_6 in case c.

The conclusion obtained from this analysis is as follows. It never happened that J_3 and J_4 are large in the case b and that J_7 and J_8 are large in the case d. This fact indicates that the destructive interference between the channels does not happen in each route. The destructive interference happens between the two routes in Figure 5. On the other hand, the constructive interference between the two routes never happened. Each route can be open or closed, depending on the protein conformation. The mechanism by which the route is open or closed will be due to the interaction between the channels. This kind of study is to be made hereafter.

4.3. Indices Representing Destructive Interference. The tunneling pathway for the electron transfer from Bph^- to Q_A in reaction centers was also investigated before.[28] By the analysis using the tube model, Balabin and Onuchic[28] found that most of the effective coupling (about 80%) is mediated by tubes through Trp^{M252} and the interference regime is primarily defined by the through-space jumps from Bph^- to Trp^{M252} and from Trp^{M252} to Q_A.[28] A weak alternative pathway (about 20% of T_{DA}^2) mediated by Met^{M218} and His^{M219} had a minor effect. From the calculated value of C, which is close to 1, they concluded that this system has a constructive interference.[28]

Our results differ from these results as follows. In our result, the contribution of the tunneling route through Met^{M218} to the total electron tunneling is a similar amount to that through Trp^{M252}. The origin of the difference will be partly due to the restriction of atomic motions in the MD simulation in the previous work.[28] Namely, all of the backbone atoms were fixed and all of the other heavy atoms were pulled to their positions in the crystallographic structure by harmonic restraining forces in their calculations. Under such a restriction, the conformation change of Met^{M218} will be much reduced, while the conformation change of Trp^{M252} will not be much affected due to the rigid structure of the residue. According to our result, the conformation fluctuation of Met^{M218} and His^{M219} produces another significant tunneling route. The other origin of the difference will be the different molecular size of donor and acceptor from ours. In the previous work, the π-conjugated regions of Bph and Q_A were chosen as the donor and the acceptor while we have chosen as the donor the and acceptor to include the σ bond regions as shown Figure 1. The significant effect of the molecular size of donor and acceptor on T_{DA} was discussed before.[13] Once the Met route is active as well as the Trp route, a possibility that the interference between the Met route and the Trp route emerges. We have shown in Figure 7A that the sign of T_{DA} for the Trp route is mostly positive and the sign of T_{DA} for the Met route is mostly negative. Therefore, if one takes an ensemble average of T_{DA} of the Trp route, then it cancels to a large extent with that of the Met route. This will be a major origin of the fact that our calculated coherence parameter C becomes much smaller than 1 for the three amino acid system and 60 amino acid system and essentially differs from the result of Balabin and Onuchic in which the value of C was close to 1.[28] Our result suggests that this system has destructive interference, according to the definition of Balabin and Onuchic. In the following, we reexamine whether the coherence parameter C itself represents properly the quantum mechanical interference effect in the electron tunneling.

To make the point of discussion clear, let us consider the case of destructive interference, which is a typical phenomenon of quantum mechanics in an electron tunneling problem. As we have seen in the present study, the sign of T_{DA} for the Trp route is opposite to that for the Met route. The destructive interference occurs when both routes are used simultaneously. This phenomenon looks like the famous diffraction pattern due to interference effect on the screen when an electronic wave passes through two slits simultaneously. When the destructive interference works, Q becomes large, and $|T_{DA}|$ becomes small. A typical example of the destructive interference was represented by a map of interatomic tunneling currents in Figure 5. When the two routes have opposite directions for tunneling currents, the sign of T_{DA} changes alternatively, and the coherence parameter C becomes small because $\langle T_{DA} \rangle$ becomes small due to almost complete cancellation of T_{DA} for the Trp route and T_{DA} for the Met route. Therefore, one may say that C is usable to judge the destructive interference.

Here, it should be pointed out that there is the following assumption for the parameter C defined by Balabin and Onuchic[28] to be used as an index of coherent interference among tunneling tubes. If the amplitude of T_{DA} for each tube is changed with the protein conformation, then the parameter C in eq 5 does not represent the interference property alone. In order that the parameter C may work as a coherence index, it must be guaranteed that T_{DA} obtained for each tube is not significantly changed by the conformation fluctuation of the protein. With regard to this point, Figure 6, parts C and D, show that the $|T_{DA}|$ values of the Trp and Met routes change by about 1 order of magnitude even in the densely distributed region. If we suppose that the tube can be substituted by the route in this system, then the condition that T_{DA} of each tube remains the same is not satisfied. Reflecting this situation, the calculated value of C in Table 1 is 0.752 for the Trp tube (route) and 0.618 for the Met tube (route). The calculated value of C for each tube (route) is considerably less than 1, although it is not much less than 1. If the tube is chosen as an atomic group with smaller size than the route in this system, then the situation will not change so much. These results indicate that the parameter C roughly reflects the coherence property, but it is modified by the fluctuation of the amplitude of T_{DA} for each tube.

4.4. Miscellaneous. As we have seen, the value of T_{DA} depends greatly on the protein conformation. Therefore, the Condon approximation is largely broken. We should adequately incorporate this feature of the Born−Oppenheimer approximation into the calculation of the electron-transfer rate. Since the electronic factor is strongly coupled with the nuclear factor, we should treat both factors in a combined way, without decoupling them. After its treatment, we should take an ensemble average for the protein conformation. By such a procedure, we obtain a new formula for the electron-transfer rate. This analysis is made in the second paper in this series of study.

In the present study, an extended Hückel theory was used for the calculation of the electronic state of the protein media. We found that a few amino acids almost substitute for the role of 60 amino acids. Under such a situation, we can use a more advanced theory of quantum chemistry for the calculation of the protein media. This kind of study will be made in future.

Among the three amino acids Trp^{M252}, Met^{M218}, and His^{M219}, which played a significant role as a mediator for the electron transfer from Bph^- to Q_A in *Rhodobactor* (*Rb.*) *sphaeroides*, two amino acids Trp^{M252} and His^{M219} are conserved in the reaction center of *Rhodopseudomonas* (*Rps.*) *viridis*[50] (PDB code 1PRC) and in the PSII of *Cyanobacterium Thermosynechococcus elongatus*[51] (PDB code 1S5L). The amino acid Met^{M218} is replaced by Ala in the reaction center of *Rps. viridis* and by Ile in the PSII of the *Cyanobacterium*. The residue of Ile is similar in size to Met. Then, Ile in the PSII of *Cyanobacterium* is located at the similar positions to that of *Rb. sphaeroides*, allowing the cofactors Phe and Q_A and the amino acids Trp and His to locate at almost the similar places to those of *Rb. sphaeroides*. The residue of Ala in the reaction center of *Rps. viridis* is much smaller than Met. On the contrary, menaquinone, which is the primary quinone Q_A of *Rps. viridis*, is considerably larger than ubiquinone, which is the Q_A of *Rb. sphaeroides*. Under these situations, the positions of some amino acids and Q_A are considerably changed from those of *Rb. sphaeroides*. It is interesting to see whether the two dominant routes are still reserved for the electron transfer from Bph^- to Q_A in *Rps. viridis*, in the similar way as we have seen in this study. This kind of study is made hereafter.

5. Conclusion

We theoretically analyzed the mechanism of the electron transfer from Bph^- to Q_A in reaction center, by taking into account conformational fluctuations of the protein media, which are produced by the MD simulation. We found that the electron tunneling matrix element T_{DA} fluctuates very quickly (in less than 50 fs) by changing its sign and amplitude drastically. One of the results in this study is the finding that the two dominant electron tunneling routes called the Trp route and the Met route exist. The Trp route and the Met route are used alternatively or simultaneously during the protein conformation fluctuation. When the Trp route is used dominantly, the sign of T_{DA} is positive. When the Met route is used dominantly, the sign of T_{DA} is negative. When the two routes are used simultaneously, the overall electron tunneling matrix element is reduced very much due to the destructive interference among the tunneling currents in the two routes.

The second result of this study is that we found that a correlation exists between $|T_{DA}|$ and the degree of destructive interference Q. More exactly, $|T_{DA}|$ is proportional to Q^{-1}. We found that Q and $|T_{DA}|$ can vary over 3 orders of magnitude due to the thermal fluctuation of protein conformation. We showed that the constructive or destructive interference is more directly described with the use of Q than the coherence parameter C, because Q is defined by considering the phase relation among the electron tunneling currents in each map, while C is defined by taking the ensemble average of the T_{DA} values among various maps. The similar linear relationship between $|T_{DA}|$ and Q^{-1} was also found before for the electron transfer in the derivatives of ruthenium-modified azurins, suggesting that this linear relationship is universal for the electron transfer through protein media. One of the important suggestions obtained from this relationship is that the electron tunneling matrix element cannot exceed a maximum value corresponding to $Q = 1$. This maximum value is determined mostly by the donor−acceptor distance and partly by the secondary structure of the protein and its arrangement.

On the basis of these results, we conclude that the mechanism of the electron transfer in protein media alternates between constructive interference and destructive interference, in the course of thermal fluctuation of the protein conformation. It is impossible to keep a system in either constructive or destructive interference, so far as the thermal fluctuation of protein conformation takes place.

Acknowledgment. This work was supported by a Grant-in-Aid on Scientific Research (C) to T.K. from the Ministry of Education, Culture, Sports, Science and Technology of Japan. This work was also supported by Grants-in-Aid on Scientific Research on the priority area "Genome Information Science" to T.Y. from the Ministry of Education, Culture, Sports, Science and Technology of Japan.

References and Notes

(1) Devault, D. *Quantum Mechanical Tunneling in Biological Systems*; Cambridge University Press: Cambridge, 1984.
(2) Marcus, R. A.; Sutin, N. *Biochim. Biophys. Acta* **1985**, *811*, 265.
(3) Siddarth, P.; Marcus, R. A. *J. Phys. Chem.* **1990**, *94*, 8430.
(4) Siddarth, P.; Marcus, R. A. *J. Phys. Chem.* **1992**, *96*, 3213.
(5) Siddarth, P.; Marcus, R. A. *J. Phys. Chem.* **1993**, *97*, 13078.
(6) Newton, M. D. *Chem. Rev.* **1991**, *91*, 767.
(7) Skourtis, S. S.; Beratan, D. N. *Electron Transfer: From Isolated Molecules to Biomolecules*; Jortner, J., Bixon, M., Eds.; John Wiley & Sons: New York, 1999; part 1, p 377.
(8) Stuchebrukhov, A. A. *J. Chem. Phys.* **1996**, *105*, 10819.
(9) Stuchebrukhov, A. A. *J. Chem. Phys.* **1997**, *107*, 6495.
(10) Gehlen, J. N.; Daizadeh, I.; Stuchebrukhov, A. A.; Marcus, R. A. *Inorg. Chim. Acta* **1996**, *243*, 271.
(11) Okada, A.; Kakitani, T.; Inoue, J. *J. Phys. Chem.* **1995**, *99*, 2946.
(12) Stuchebrukhov, A. A. *Advances. in Chemical Physics*; Prigogine, I., Rice, S. A., Eds.; John Wiley & Sons: New York, 2001; Vol. 118, p 1.
(13) Kawatsu, T.; Kakitani, T.; Yamato, T. *J. Phys. Chem. B* **2002**, *106*, 5068.
(14) Beratan, D. N.; Onuchic, J. N.; Hopfield, J. J. *J. Chem. Phys.* **1987**, *86*, 4488.
(15) Onuchic, J. N.; Beratan, D. N.; Winkler, J. R.; Gray, H. B. *Annu. Rev. Biophys. Biomol. Struct.* **1992**, *21*, 349.
(16) Betts, J. N.; Beratan, D. N.; Onuchic, J. N. *J. Am. Chem. Soc.* **1992**, *114*, 4043.
(17) Regan, J. J.; Bilio, A. J. D.; Langen, R.; Skov, L. K.; Winkler, J. R.; Gray, H. B.; Onuchic, J. N. *Chem. Biol.* **1995**, *2*, 489.
(18) Regan, J. J.; Onuchic, J. N. *Electron Transfer: From Isolated Molecules to Biomolecules*; Jortner, J., Bixon, M., Eds.; John Wiley & Sons: New York, 1999; part 2, p 467.
(19) de Andrade, P. C. P.; Onuchic, J. N. *J. Chem. Phys.* **1998**, *108*, 4292.
(20) Stuchebrukhov, A. A. *J. Chem. Phys.* **1996**, *104*, 8424.
(21) Stuchebrukhov, A. A. *J. Chem. Phys.* **1998**, *108*, 8499.
(22) Stuchebrukhov, A. A. *J. Chem. Phys.* **1998**, *108*, 8510.
(23) Kawatsu, T.; Kakitani, T.; Yamato, T. *J. Phys. Chem. B* **2001**, *105*, 4424.
(24) Daizadeh, I.; Medvedev, E. S.; Stuchebrukhov, A. A. *Proc. Natl. Acad. Sci. U.S.A.* **1997**, *94*, 3703.
(25) Antony, J.; Medvedev, E. S.; Stuchebrukhov, A. A. *J. Am. Chem. Soc.* **2000**, *122*, 1057.
(26) Wolfgang, J.; Risser, S. M.; Priyadarshy, S.; Beratan, D. N. *J. Phys. Chem. B* **1997**, *101*, 2986.
(27) Aquino, A. J. A.; Beroza, P.; Reagan, J. J.; Onuchic, J. N. *Chem. Phys. Lett.* **1997**, *275*, 181.
(28) Balabin, I. A.; Onuchic, J. N. *Science* **2000**, *290*, 114.
(29) Xie, Q.; Archontis, G.; Skourtis, S. S. *Chem. Phys. Lett.* **1997**, *312*, 237.
(30) Kawatsu, T.; Kakitani, T.; Yamato, T. *J. Phys. Chem. B* **2002**, *106*, 11356.
(31) Kobayashi, C.; Baldrige, K.; Onuchic, J. N. *J. Chem. Phys.* **2003**, *119*, 3550.
(32) Tan, M.-L.; Balabin, I. A.; Onuchic, J. N. *Bio. Phys.* **2004**, *86*, 1813.
(33) Stowell, M. H. B.; McPhillips, T. M.; Rees, D. C.; Soltis S. M.; Abresch, E.; Feher, G. *Science* **1997**, *276*, 812.
(34) Saito, M. *Mol. Simul.* **1992**, *8*, 321.
(35) Morikami, K.; Nakai, T.; Kidera, A.; Saito, M.; Nakamura, H. *Comput. Chem.* **1992**, *16*, 243 (PRESTO, a vectorized molecular mechanics program for biopolymers).

(36) Cornell, W. D.; Cieplak, P.; Bayly, C. I.; Gould, I. R.; Merz, K. M., Jr.; Ferguson, D. M.; Spellmeyer, D. C.; Fox, T.; Caldwell, J. W.; Kollman, P. A. *J. Am. Chem. Soc.* **1995**, *117*, 5179.

(37) Howell, J.; Rossi, A.; Wallace, D.; Haraki, K.; Hoffmann, R. *QCPE* **1977**, *11*, 344 (FORTICON8, extended Hückel method program).

(38) Kincaid, D. R.; Respess, J. R.; Young, D. M.; Grimes, R. G. *ITPACK 2C*; University of Texas: Austin, TX, 1999 (a fortran package for solving a large sparse linear system by adaptive accelerated iterative methods).

(39) Stewart, J. J. P. *J. Comput. Chem.* **1989**, *10*, 209.

(40) Frisch, M. J.; Trucks, G. W.; Schlegel, H. B.; Scuseria, G. E.; Robb, M. A.; Cheeseman, J. R.; Zakrzewski, V. G.; Montgomery, J. A., Jr.; Stratmann, R. E.; Burant, J. C.; Dapprich, S.; Millam, J. M.; Daniels, A. D.; Kudin, K. N.; Strain, M. C.; Farkas, O.; Tomasi, J.; Barone, V.; Cossi, M.; Cammi, R.; Mennucci, B.; Pomelli, C.; Adamo, C.; Clifford, S.; Ochterski, J.; Petersson, G. A.; Ayala, P. Y.; Cui, Q.; Morokuma, K.; Malick, D. K.; Rabuck, A. D.; Raghavachari, K.; Foresman, J. B.; Cioslowski, J.; Ortiz, J. V.; Baboul, A. G.; Stefanov, B. B.; Liu, G.; Liashenko, A.; Piskorz, P.; Komaromi, I.; Gomperts, R.; Martin, R. L.; Fox, D. J.; Keith, T.; Al-Laham, M. A.; Peng, C. Y.; Nanayakkara, A.; Challacombe, M.; Gill, P. M. W.; Johnson, B.; Chen, W.; Wong, M. W.; Andres, J. L.; Gonzalez, C.; Head-Gordon, M.; Replogle, E. S.; Pople, J. A. *Gaussian 98*, revision A.9; Gaussian, Inc.: Pittsburgh, PA, 1998.

(41) Stuchebrukhov, A. A. *Chem. Phys. Lett.* **1994**, *225*, 55.

(42) Stuchebrukhov, A. A.; Marcus, R. A. *J. Phys. Chem.* **1995**, *99*, 7581.

(43) Kawatsu, T.; Kakitani, T.; Yamato, T. *Inorg. Chim. Acta* **1997**, *300*−*302*, 862.

(44) Humphrey, W. F.; Dalke, A.; Schulten, K. J. *J. Mol. Graphics* **1996**, *14*, 33.

(45) Schwartz, B. J.; Bittner, E. R.; Prezhdo, O. V.; Rossky, P. J. *J. Chem. Phys.* **1996**, *104*, 5942.

(46) Prezhdo, O. V.; Rossky, P. J. *J. Chem. Phys.* **1997**, *107*, 5863.

(47) Moser, C. C.; Keske, J. M.; Warnucke, K.; Farid, R. S.; Dutton, P. L. *Nature* **1992**, *355*, 796.

(48) Page, C. C.; Moser C. C.; Chen, X.; Dutton, P. L. *Nature* **1999**, *402*, 47.

(49) Gray, H. B.; Winkler, J. R. *Annu. Rev. Biochem.* **1996**, *65*, 537.

(50) Deisenhofer, J.; Epp, O.; Sinning, I.; Michel, H. *J. Mol. Biol.* **1995**, *246*, 429.

(51) Ferreira, K. N.; Iverson, T. M.; Maghlaoui, K.; Barber, J.; Iwata, S. *Science* **2004**, *303*, 1831.